Journal of Applied Polymer Science

Characterization of p(AA-co-AM)/bent/urea and its swelling and slow release behavior in a simulative soil environment

Peng Wen, Zhansheng Wu, Yanhui He, Yajie Han, Yanbin Tong
School of Chemistry and Chemical Engineering, Shihezi University, Shihezi, 832003, People's Republic of China
Correspondence to: Z. Wu (E-mail: wuzhans@126.com)

ABSTRACT: In this work, a novel slow release fertilizer contained 14.98% nitrogen was prepared via free radical polymerization of acrylic acid, acrylamide, and bentonite in the presence of cross-linker (*N*,*N*′-methylenebis acrylamide), initiator (potassium persulfate), and nutrient source (urea). The samples were analyzed using a Fourier transform infrared spectrometer, X-ray diffraction, Scanning electron microscopy, Thermogravimetric analysis, and Brunauer, Emmett and Teller analysis. Results showed that the swelling and release behaviors were strongly dependent on the type and concentration of salt solution added to the medium, pH levels of the solutions, and temperature. Moreover, the experimental data indicated that the addition of Bent not only improved water absorbency and water retention capacities but also controlled the release of nutrients. The release kinetic simulation analysis findings showed that the release of urea was predominated by a Case II release mechanism with skeleton erosion. © 2015 Wiley Periodicals, Inc. J. Appl. Polym. Sci. **2016**, *133*, 43082.

KEYWORDS: applications; clay; composites; porous materials; stimuli-sensitive polymers

Received 16 July 2015; accepted 26 October 2015
DOI: 10.1002/app.43082

INTRODUCTION

Fertilizers and water resources are the most important factors for the agricultural production, and they are commonly considered as being yield limiting, so it is very necessary to improve the utilization of fertilizer nutrients and water resources.[1] However, conventional fertilizers used in agriculture, horticulture, and related fields dissolve quickly. Thus, such fertilizers cannot be utilized efficiently by plants. The loss of fertilizer not only negatively causes the economic losses but also leads to very serious health and environmental problems, such as the contamination with water, air, and so forth.[2] To mitigate these problems, slow release fertilizers (SRFs) have been designed and applied in various fields. These novel fertilizers can release nutrients gradually to coincide with the nutrient requirements of plants, thus can make it available in the field for a longer period than conventional fertilizers.[3,4] Studies that have replaced the conventional fertilizers with SRFs have reported encouraging results, SRFs not only help limit fertilizer loss and enhance fertilizer utilization efficiency but also address the contamination caused by common fertilizers. Wu *et al.* synthesized a double-coated slow release nitrogen, phosphorus, and potassium (NPK) fertilizer with slow release property and excellent water-retention capability that is superior to that of conventional fertilizers. Therefore, this NPK fertilizer would be used widely in various fields.[5]

The shortage of water resources is one of the most severe problems in the 21st century, especially in arid and semiarid regions. Moreover, the effective utilization of scarce water resources is a major challenge for farmers and has aroused wide concern in the public.[6] For the purpose of improving the utilization ratio of water resources and limiting irrigation frequency, a growing number of researchers has devoted themselves to investigating the use of superabsorbent polymers (SAP) as water management materials for agricultural applications.[1,4,5] SAP are slightly cross-linked hydrophilic polymers capable of swelling and retaining considerable amounts of water or physiological fluids by virtue of the unique three-dimensional network structure and various functional groups without undergoing dissolution.[4,7,8] The use of SAP improves the water-holding capacity and fertility of the soil.[4,7] However, the majority of available SAP are mainly based on synthetic hydrophilic polymers such as p(acrylic acid) or its copolymer with p(acrylamide), the high cost and poor degradability in soil ends up making its application unfeasible and limiting the extensive application in various fields.[4,9] To solve these problems, one of the alternatives is to introduce inorganic clays such as montmorillonite (MMT), bentonite (Bent), attapulgite, kaolin, and mica in high proportions into pure SAP to form the organic-inorganic superabsorbent due to its good degradability and low cost.[1,4,7] It has been found that the inclusion of nature clay minerals not only reduces production costs drastically but also improves some of its properties, like swelling ability, gel strength, and mechanical and thermal stability.[4,7,10] Bent is a low-cost natural clay material that possesses unique

physical and chemical properties, such as the typical 2:1 layered structure, high cation exchange capacity, reactive groups on its surface, the capability to densify polymeric network structures, and the capability to affect slow release property, it has been widely used in agricultural applications because of these characteristics.[6] Recent works by Bhattacharya *et al.*[11] showed that the introduction of modified Bent not only effectively increases water absorbency, but also improves water retention ability. However, the study on the synthesis of organic–inorganic SRF on the basis of acrylic acid (AA), acrylamide (AM), Bent, and urea as raw materials via inversion suspension polymerization has not been reported. Thus, to develop such SRF and explore their swelling and slow release behavior in response to external stimuli, namely, salt solutions, temperature, and pH by stimulating soil environment is of importance, which is very useful for potential agriculture and horticulture applications.

In this work, a novel SRF with good slow-release and water-absorbency properties based on AA, AM, Bent, and urea with potassium persulfate (KPS) and *N,N′*-methylenebis acrylamide (MBA) as initiator and crosslinker were synthesized. The synthesized samples were characterized using a Fourier transform infrared spectrometer (FTIR), X-ray diffraction (XRD), Scanning electron microscopy (SEM), Thermogravimetric analysis (TGA), and Brunauer, Emmett, and Teller analysis (BET). Moreover, differences in soil texture, pH levels, and application temperatures among various regions exert a significant effect on swelling and nutrient release behavior. Typical cationic saline solutions in soil (such as NaCl, $MgCl_2$, $CaCl_2$, $BaCl_2$, and $FeCl_3$), different pH levels and varying temperatures are considered to investigate the effect of environment factors on the swelling and release behavior. The release kinetics of the synthesized sample was also provided. Therefore, the current study is significant to SRFs production and application and could be expected to be widely applicable in modern agriculture and horticulture.

EXPERIMENTAL

Materials

AA and cyclohexane were provided by Tianjin Fuyu Fine Chemical (China). AA was distilled under reduced pressure before use to remove the polymerization inhibitor and stored in a brown reagent bottle. KPS (Tianjin Shengao Chemical Industry Limited Company, Tianjin, China) was recrystallized from water prior to use. AM was purchased from Tianjin Fuchen Chemical Reagent (China). MBA was obtained from Tianjin Institute of chemical reagents (China). Urea and sorbitan monostearate (span 60) was supplied by Chengdu Kelong Chemical Reagent Factory (China). Dimethylaminobenzaldehyde was from Linshu Xiya Chemical Industry (China). All reagents were of analytical grade and all solutions were prepared with distilled water. The raw Bent samples were collected from XiaZiJie deposits in Xinjiang Uyghur Autonomous Region of China. The Bent used was purified using the method of Sun *et al.*[12] The cation exchange capacity was 98.4 mmol based on 100 g Bent and the swelling index was 89.5 mL g^{-1}.

Preparation of P(AA-co-AM)/Bent/Urea

Preparation of P(AA-co-AM)/Urea Formulation. 5.0 g of AA was dissolved in 20 mL of distilled water under gentle stirring, and then it was partially neutralized with a certain amount of sodium hydroxide solution in an ice bath up to the 70% neutralization degree. Afterward, 5.0 g of AM, 3.6 g of urea, 1.2 mL of 0.01 mol L^{-1} MBA, and 4.0 mL of 0.04 mol L^{-1} KPS were added into the monomer solution, successively, and stirred for 30 min at a constant speed of 300 rpm until the mixture was uniform. After the reaction completed, the water phase was prepared.

Moreover, 60 mL of cyclohexane was poured into a 250 mL four-necked flask equipped with a mechanical stirrer, reflux condenser, a thermometer, and a nitrogen line, and then 1.2 g of span 60 was slowly added and stirred at 300 rpm for a few minutes at 40°C in a water bath to have span 60 dissolved completely. When the process accomplished, the oil phase was obtained.

As stirring continued, the water phase was charged into oil phase flask dropwise according to the volume ratio of 1:3. After being purged with nitrogen gas for a few minutes to get rid of dissolved oxygen in the solution, the water bath was heated slowly to 70°C and last for 2.18 h on the basis of our previous work. The polymerization was completed under nitrogen atmosphere while stirring at a constant speed of 500 rpm. When the reaction completed, the suspension solution was filtrated after it cooled to room temperature. The production was purified with 70% of ethanol and dried to constant weight in a vacuum oven at 70°C. Finally, the brown granular p(AA-co-AM)/Urea was obtained and stored for further use.

Preparation of P(AA-co-AM)/Bent/Urea Formulation. The preparation procedure was exactly similar to that described previously with a little difference that 1.0 g of Bent was added into the monomer solutions in the process of prepare water phase and make the Bent dispersed uniformly. In continue a same method mentioned above was adopted to synthesize the p(AA-co-AM)/Bent/Urea formulation.

Characterization Methods

FTIR Analysis. The spectroscopic characterization of the samples was investigated using a FTIR spectrometer (Nicolet Avatar 360). The samples of Bent, urea, p(AA-co-AM)/Bent, p(AA-co-AM)/Urea, and p(AA-co-AM)/Bent/Urea were completely dried, grounded to fine powder, and mixed thoroughly with KBr and pressed forming KBr tablets, respectively. The FTIR spectra of the samples were then recorded in the wave number range of 4000–400 cm^{-1}.

SEM Analysis. The surface morphologies of the p(AA-co-AM)/Urea and p(AA-co-AM)/Bent/Urea were studied using a SEM (JSM-6700F, Jeol, Tokyo, Japan). The samples were dried and adhered to sample holders with carbon LIT-C glue, and their surfaces covered with a gold thin layer to prevent the collapse of the porous structure.

XRD. The structural properties of Bent, p(AA-co-AM)/Bent, p(AA-co-AM)/Urea, and p(AA-co-AM)/Bent/Urea were analyzed using a XRD (D8 Advance, Bruker) with Cu kα ($\lambda = 1.54056$) radiation at room temperature, operating with an emission tube acceleration voltage of 40 kV, current of 40 mA. The scanning velocity used was 1.0° min^{-1} and the samples were scanned in the angle range of 5–90°.

Thermogravimetric Analysis. The TG properties of Bent, urea, p(AA-co-AM)/Urea and p(AA-co-AM)/Bent/Urea were carried out using a TGA (STA 449F3, NETZSCH, Germany) with a

temperature range of 25–800°C at a heating rate of 10°C min^{-1} using dry nitrogen purge at a flow rate of 30 mL min^{-1}.

BET Measurement. The pore volume, pore size distribution, and specific surface area of p(AA-co-AM)/Urea and p(AA-co-AM)/Bent/Urea were measured using an Accelerated Surface Area and Porosimetry System (ASAP2020, Micromeritics, America) that uses a nitrogen adsorption-desorption method at 77 K. The specific surface area was calculated using BET equation.

Swelling Measurement

About 0.1 g of the pre-dried samples were immersed entirely in 250 mL of distilled water, various saline solutions (NaCl, $MgCl_2$, $CaCl_2$, $BaCl_2$, and $FeCl_3$) with different concentration ranging from 0.05 to 0.25 mol L^{-1} and various pH value solutions ranged from 2.0 to 12.0 at room temperature until the swelling equilibrium was reached. The swollen samples were filtered through a 100-mesh stainless screen and weighed. The equilibrium water absorbency Q_{eq} (g g^{-1}) was calculated by eq. (1).

$$Q_{eq} = \frac{W_2 - W_1}{W_1} \quad (1)$$

where W_1 and W_2 are the weights of dried and swollen product, respectively. Q_{eq} was expressed as grams of water uptake by per gram of sample.

To explore the effect of temperature on water absorbency, pre-dried samples were immersed in distilled water and then put into incubators whose temperature was set at 5, 25, and 35°C. The measurement of water absorbency was the same as described previously.

Determination of the Urea Content

The quantity of cumulative urea released from the samples in the solutions was determined using a simple spectrophotometric method proposed by With *et al.*[13] Aliquot (5 mL) was pipetted into a 25 mL colorimetric tube, and then 10 mL of Ehrlich reagent was added. Subsequently, the solution was diluted into 25 mL with distilled water and renewed mixing gently. Dimethylaminobenzaldehyde gradually reacted with the urea and generated a bright yellow color complex that was proportional to urea concentration under acidic conditions. This color complex was quantified by photometry. The absorbance values of the mixture were measured with a blank using a UV−vis spectrophotometer (752 N, METASH, China) at a wavelength of 430 nm after 10 min. The mechanism of this method is according to the following reaction:

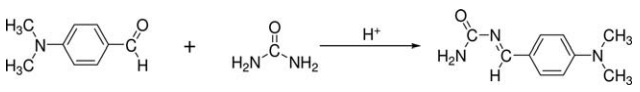

The amount of urea released at different time intervals was determined by measuring the absorbance value of the aliquots at desired time intervals. The absorbance value is related to the amount of urea identified as per a calibration plot ($y = 3.0221x - 0.0059$). Finally, the curve of urea cumulative release ratio versus release time was obtained.

Slow Release Kinetics and Mechanisms

The slow-release property of the samples can be described as the cumulative urea release. 0.1 g of the pre-dried samples were immersed in 250 mL of distilled water, various saline solutions (0.05, 0.15, and 0.25 mol L^{-1} NaCl, 0.05 mol L^{-1} $MgCl_2$, $CaCl_2$, $BaCl_2$, and $FeCl_3$) and aqueous solution with well-defined pH values of 4, 7, and 9. During 30 days at room temperature, aliquots (5 mL) were collected at certain time intervals for analysis and the same volume of fresh medium was supplemented to maintain a constant amount of solvent. The urea content released from the samples was determined according to the colorimetric determination described previously.

To explore the effect of temperature on slow release behavior, pre-dried samples were added into beakers containing 250 mL distilled water, and then put into incubators whose temperature was set at 5, 25, and 35°C. The measurement of urea content was the same as described previously.

With the aim of revealing the slow release kinetics and mechanism, the release data into medium were fitted to the empirical eq. (2) proposed by Ritger and Peppas[14]:

$$\frac{M_t}{M_\infty} = kt^n \text{ or } \ln(M_t/M_\infty) = \ln k + n\ln(t) \quad (2)$$

where M_t/M_∞ is the fraction of urea released at time t, k is the rate constant that incorporates characteristics of the carrier and the active ingredient, and n is the release exponent which defines the transport mechanism. The value of n is determined from the slope of the plot of the ln (M_t/M_∞) versus ln (t) and the diffusion constant k was obtained from the intersection with the vertical axis.

Measurement of the Water Retention of Samples

The water retention of samples at different temperatures was studied as follows: the samples were soaked in distilled water until the equilibrium at room temperature, then a certain quantity of fully swollen samples (marked W_1) were placed in an air oven at 45 and 80°C, respectively. The remaining samples were weighed at different time intervals (marked W_i). The water-retention ratio (WR %) of the samples were calculated by eq. (3).

$$WR(\%) = \frac{W_i}{W_1} \times 100 \quad (3)$$

RESULTS AND DISCUSSION

Preparation Mechanism of P(AA-co-AM)/Bent/Urea

The p(AA-co-AM)/Bent/Urea product was prepared via free radical reaction. The specific procedure is described as follows[7]: first, the sulfate anion radicals were generated from the thermal decomposition of the persulfate initiator. Second, these radicals attacked the monomer molecules of AA and AM that were adjacent to the active centers resulting in chain initiation. Thereafter, the chain propagation began rapidly and led to the growth of a branched chain subsequently. Finally, the cross-linked network structure was formed via the reaction between the end vinyl groups of MBA crosslinker and the polymer chains. In addition, it is clear that the Bent may act as a cross-linking agent to form the network and the urea dispersed uniformly in the network.

Characterization

FTIR Spectra. The FTIR spectra of the Bent, urea, p(AA-co-AM)/Bent, p(AA-co-AM)/Urea, and p(AA-co-AM)/Bent/Urea

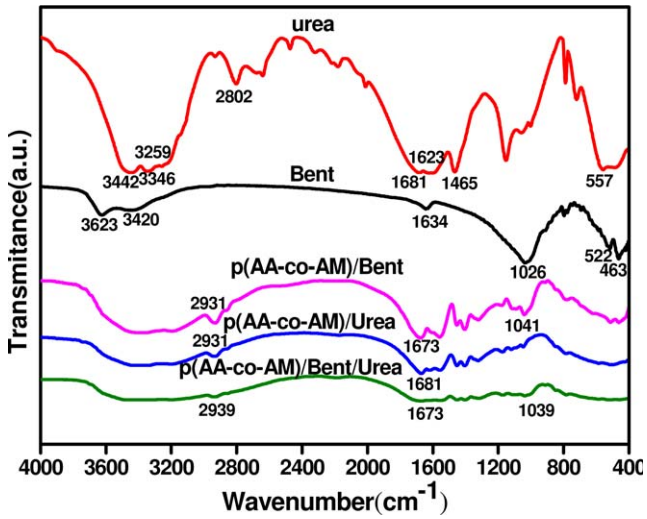

Figure 1. The FTIR spectra of the Bent, urea, p(AA-co-AM)/Bent, p(AA-co-AM)/Urea, and p(AA-co-AM)/Bent/Urea. [Color figure can be viewed in the online issue, which is available at wileyonlinelibrary.com.]

were shown in Figure 1. In FTIR spectra of Bent, the absorption bands at 1634 and 787 cm^{-1} were related to O—H bending vibration and the peak observed at 3420 cm^{-1} was associated with stretching vibration of structural O—H, the band at 522 cm^{-1} was corresponded to the Al—O—Si bending vibration.[15] It was worth to mention that the Al—OH and Mg—OH stretching vibration of Bent at 3623 cm^{-1} can almost not be observed, the Si—O stretching vibration at 1026 cm^{-1} and the Si—O—Si bending vibration at 463 cm^{-1} can be observed in p(AA-co-AM)/Bent and p(AA-co-AM)/Bent/Urea with a weakened intensity, indicating that Bent participated in polymerization reaction. In FTIR spectra of urea, the peaks at 3442 and 3346 cm^{-1} were corresponded to asymmetric and symmetric stretching vibration of NH_2.[16] The peak at 3259 cm^{-1} was due to O—H vibration of absorbed water, 2802 cm^{-1} was identified as C—H of formaldehyde in the urea.[17] The peak that appeared at 1681 cm^{-1} was attributed to C═O groups stretching, 1623 and 1465 cm^{-1} were corresponded to N-H bending vibration and C—N stretching vibration,[16] 557 cm^{-1} was related to N—CO—N bending vibration,[18] and these peaks still existed in p(AA-co-AM)/Urea and p(AA-co-AM)/Bent/Urea, which indicated the involvement of urea in the samples and the chemical structure of the urea is stable. In FTIR spectra of p(AA-co-AM)/Bent, p(AA-co-AM)/Urea, and p(AA-co-AM)/Bent/Urea, the bands at 1673, 1681, and 1673 cm^{-1} were related to the overlapped stretching vibration of the C═O groups of AA and AM as well as the N—H bending.[19] The bands appeared at 2931, 2931, and 2939 cm^{-1} were due to the combined stretching of CH_2 groups in both AA and AM in superabsorbent structure.[4]

XRD Patterns. The XRD patterns of Bent, p(AA-co-AM)/Bent, p(AA-co-AM)/Urea, and p(AA-co-AM)/Bent/Urea were shown in Figure 2. It can be observed that the crystalline peak of Bent at 8.90° disappeared in the XRD patterns of p(AA-co-AM)/Bent and p(AA-co-AM)/Bent/Urea, suggesting the reaction between the Bent and monomers weakened the ordered structures of Bent and the clay sheets of the Bent have been exfoliated during the reaction and then uniformly dispersed in organic network.[9] Furthermore, the presence of the characteristic diffraction peaks of Bent in the XRD pattern of p(AA-co-AM)/Bent and p(AA-co-AM)/Bent/Urea confirmed the incorporation of the Bent in the p(AA-co-AM)/Bent and p(AA-co-AM)/Bent/Urea. In addition, it was worthy noted that p(AA-co-AM)/Bent and p(AA-co-AM)/Bent/Urea possess typical crystallite reflections associated with the MMT component, while the XRD patterns of p(AA-co-AM)/Urea present two weak broad peaks at $2\theta = 22°$ and $2\theta = 38°$ attributed to its amorphous structure with low crystallinity.[4]

SEM Surface Morphology. The SEM images of the SRFs with and without the Bent were shown in Figure 3. It can be seen that urea crystals is homogeneously deposited on the surface of polymer in a lower magnification. For clarification, some of the urea crystals were shown by arrow signs in SEM images. Furthermore, in a higher magnification, the SEM clearly indicates that the p(AA-co-AM)/Urea had comparatively smooth, tight surfaces and less porous structure in contrast to p(AA-co-AM)/Bent/Urea, which has an undulant, course surface and more pores and open channels with honeycomb-like structure due to the introduction of the Bent, which act as the physical crosslinking agent increased the surface area and facilitated the water molecules penetrating into the polymeric network finally.

Thermogravimetric Analysis. The TGA curves of Bent, Urea, p(AA-co-AM)/Urea, and p(AA-co-AM)/Bent/Urea were depicted in Figure 4. The thermal decomposition process of urea was divided into two steps, the first step was corresponded to the urea vaporization, decomposition, and the generation of biuret, $NH(CO)_2(NH_2)_2$ as well as the decomposition and self-condensation of biuret,[20] and the second step was associated with the continuous sublimation and decomposition of the urea

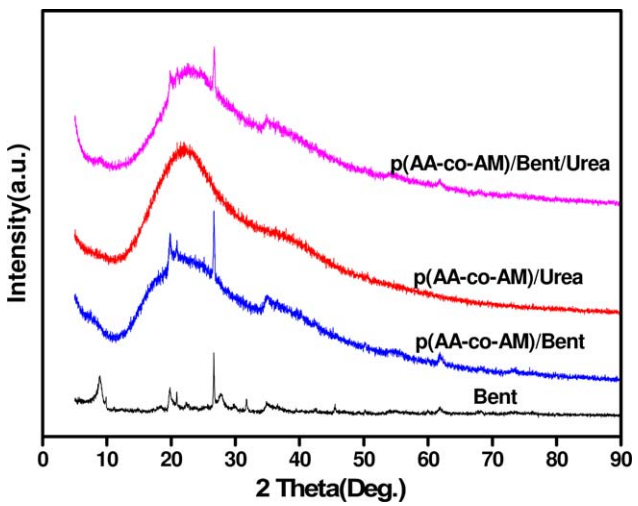

Figure 2. X-ray diffraction patterns of the Bent, p(AA-co-AM)/Bent, p(AA-co-AM)/Urea, and p(AA-co-AM)/Bent/Urea. [Color figure can be viewed in the online issue, which is available at wileyonlinelibrary.com.]

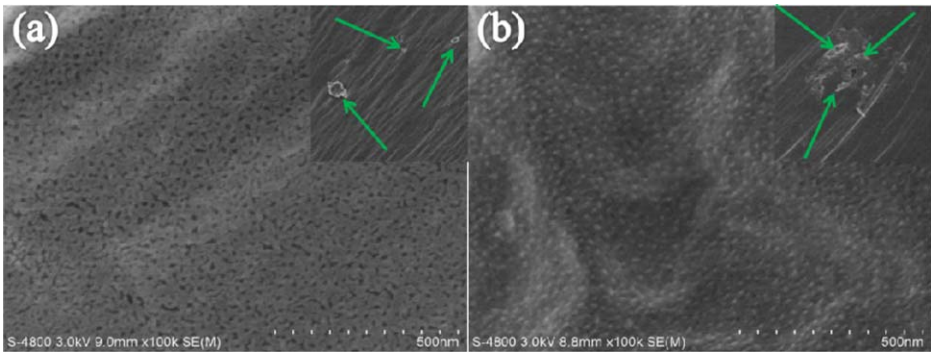

Figure 3. SEM micrographs of p(AA-co-AM)/Urea (a) and p(AA-co-AM)/Bent/Urea (b). [Color figure can be viewed in the online issue, which is available at wileyonlinelibrary.com.]

and other complex samples until complete chemical vaporization and degradation.[20] The decomposition curve of Bent showed two-steps decomposition related to dehydration of adsorbed water and interlayer water (first step),[21] and to the elimination of dehydroxylation water and organic matter (second step).[21] In addition, p(AA-co-AM)/Urea and p(AA-co-AM)/Bent/Urea possessed a similar four-steps continuous thermal decomposition process and the decomposition rate was follows the series p(AA-co-AM)/Bent/Urea < p(AA-co-AM)/Urea. The first step was due to the removal of the absorbed and bonded water in the network,[10] the second step was attributed to the thermal decomposition of amide groups, carboxyl groups of p(AA-co-AM) chains backbone and crosslinker on the network,[22] the third step was implied the formation of anhydride with elimination of the water molecule from two neighboring carboxyl groups and the breakage of p(AA-co-AM) chains as well as the destruction of cross-linked network structure,[23] the last step was assigned to the further decomposition or degradation of residual organic matter at high temperature.[23] In the end, the residual weight of p(AA-co-AM)/Bent/Urea was about 31.91%, which was higher than that about 26.61% for p(AA-co-AM)/Urea. The conclusion was easily reached that the incorporation of Bent obviously caused an increase in thermal stability of the polymer.

BET Analysis. Specific surface area and pore size distribution are important sample properties. The pore size distribution and adsorption/desorption isotherms (inset) for p(AA-co-AM)/Urea and p(AA-co-AM)/Bent/Urea were shown in Figure 5. It can be seen that both isotherms were almost similar in shape and increased sharply at low relative pressure, which is characteristic features of the Type I isotherms and indicates the existence of micropores.[24] Furthermore, a H_3 hysteresis loop, which is a remarkable characteristic of the Type IV isotherms and is associated with the capillary condensation taking place in mesopores,[24] was also observed with the increase of relative pressure. These findings indicated that both isotherms are clearly a mixture of types I and IV isotherms, suggesting the simultaneous existence of micropores and mesopores.[25] Moreover, the introduction of Bent varied the volume of N_2 adsorbed, which suggested Bent as physical crosslinking agent increased crosslinking density and pore number. That is, the BET surface area and total pore volume of p(AA-co-AM)/Bent/Urea (5.286 $m^2\ g^{-1}$ and 0.0034 $cm^3\ g^{-1}$) were twice as high as those of p(AA-co-AM)/Urea (2.352 $m^2\ g^{-1}$, 0.0016 $cm^3\ g^{-1}$). The p(AA-co-AM)/

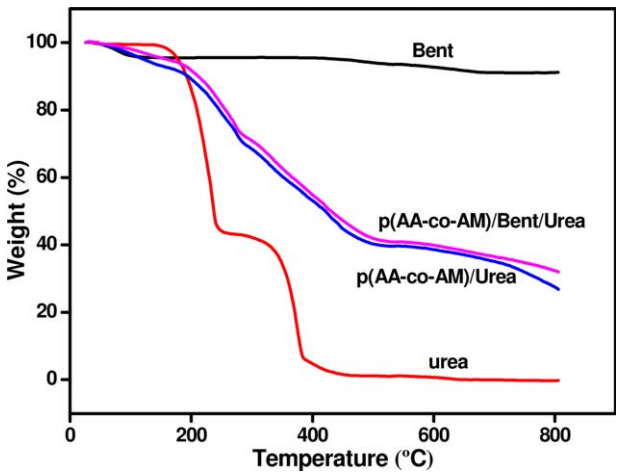

Figure 4. TG curves of the Bent, urea, p(AA-co-AM)/Urea, and p(AA-co-AM)/Bent/Urea. [Color figure can be viewed in the online issue, which is available at wileyonlinelibrary.com.]

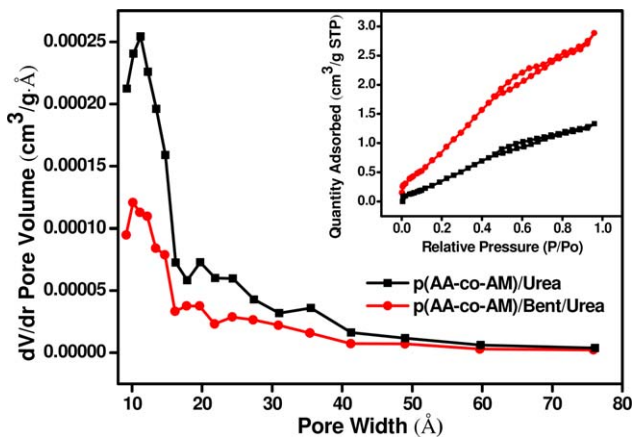

Figure 5. The pore size distributions and nitrogen adsorption/desorption isotherms (inset) for fertilizers. [Color figure can be viewed in the online issue, which is available at wileyonlinelibrary.com.]

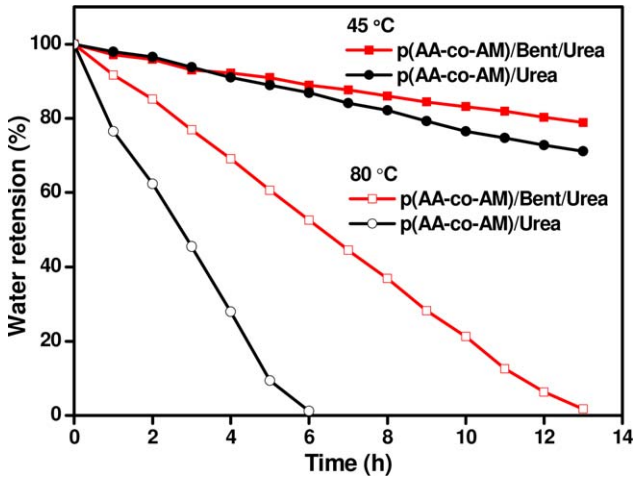

Figure 6. Water retention ability of swollen fertilizers with and without Bent as a function of time at 45 and 80°C. [Color figure can be viewed in the online issue, which is available at wileyonlinelibrary.com.]

Bent/Urea also displayed a consistent pore radius ranging from 9 to 60 Å, with an average pore size of 18.9 Å, which indicated the samples has micro-mesopores structure, corresponding to the N_2 adsorption/desorption results. The higher BET surface area and total pore volume benefited the water absorbency and release property. Rashidzadeh *et al.*[4] synthesized a Hyd/MMT/NPK fertilizer that possessed a slow-release property superior to that of fertilizer without MMT ascribed to the highly porous structure originated from the addition of MMT.

Measurement of the Water Retention of Samples

In real circumstance, not only the slow release property and the water absorbency but also the water retention of the product is of vital importance, especially in arid and desert regions. Figure 6 showed the water retention capacity of the samples as a function of time at 45 and 80°C. As clearly seen, the water retention capacity decreased with prolonging the time and the addition of Bent obviously improved the water retention capacity in contrast to p(AA-co-AM)/Urea. Under 80°C condition, the water loss of p(AA-co-AM)/Urea almost reached 100% after 6 h, while the 100% of water loss of p(AA-co-AM)/Bent/Urea reached can be delayed to 13 h. In addition, the p(AA-co-AM)/Bent/Urea and p(AA-co-AM)/Urea hold 78.9% and 71.1% of distilled water after drying for 13 h at 45°C, respectively. The H-bonding interaction and Van der Waals forces between the water molecules and the samples has a direct impact on water retention performance.[26] The inherent carboxylate groups on the network chains made this chemical interaction stronger, furthermore, the Bent has an excellent water absorbency and water retention capacity, which give rise to an improvement in the water retention capacity.[26] From the results, it could be inferred that the samples had good water retention ability, which is especially significant for the arid and desert areas. The samples would be like a subminiature reservoir to retain and supply moisture to crops over time as the soil underwent alternate wet and dry, consequently, reduce irrigation frequencies, prolong irrigation cycles, and strengthen drought resistance of crops when the samples applied in the soil, consequently, a good environment for crops to grow would be created.[3]

Influence of the Environmental Factors on Water Absorbency

Effect of Salt Solution on Water Absorbency. The effect of various ions and concentrations on the water absorbency of fertilizers was illustrated in Figure 7. It can be seen that the water absorbency of p(AA-co-AM)/Bent/Urea was always higher than that of p(AA-co-AM)/Urea and the trends of swelling behavior in all swelling media were similar. This result indicated that the introduction of Bent improved the saline resistance of fertilizers to some extent. Initially, water absorbency decreased sharply as the salt concentration of the solutions increased from 0 to 0.05 mol L^{-1} which is related to the expansion of the samples network decreased ascribed to the charge screening effect induces an imperfect anion-anion electrostatic repulsion and a reduced osmotic pressure result from the additions of these cations.[27] Second, the tendency was followed by a gradual decrease with an increase in salt concentration from 0.05 to 0.25 mol L^{-1}. This finding can be attributed to the fact that ionic osmotic pressure decreased more significantly with the cationic solution concentration increased, which in turn prevented water molecules from penetrating inside the network and limited swelling in the process.[26] As shown in Figure 7(a), the water absorbency in the NaCl solution was considerably higher than that in the $CaCl_2$ and $FeCl_3$ solutions at same concentrations, and the degree of suppression on water absorbency was ordered as follows: $Fe^{3+} > Ca^{2+} > Na^{+}$. When the cation charge increased from monovalent to multivalent, the complexing ability between metal ions and the carboxylate group increased and the electrostatic repulsive forces between the carboxylate groups weakened, which lead to the degree of crosslinking increased and the expansion of network constrained.[28] Besides, the multivalent metal cationic salt solution displayed higher ionic strength than the monovalent metal cationic salt solution.[23] As indicated in Figure 7(b), the less the radius of the same valent cation, the larger water absorbency was ($Mg^{2+} > Ca^{2+} > Ba^{2+}$). This result may be ascribed to the fact that the less the cation radius is, the more cations permeate the network. This scenario results in a favorable anion–anion electrostatic repulsion, thus improving water absorbency. Similar phenomena had been reported by others.[23,28]

Effect of pH on Water Absorbency. Swelling behavior of the samples in solutions of various pH levels that ranged from 2.0 to 12.0 was investigated. The desired pH media were adjusted using 0.05 mol L^{-1} of HCl and NaOH solutions. The pH levels were measured with a pH meter (PHS-3C). As displayed in Figure 8, the water absorbency of p(AA-co-AM)/Bent/Urea was always higher than that of p(AA-co-AM)/Urea and both samples continuously swelled up to a pH level of 8 and then decreased with further increases in pH level, the water absorbency of the hydrogels was maximized at pH 8. At low pH, the water absorbency of both samples decreased, this result may be attributed to the fact that most carboxylate anions were protonated under acidic conditions, as a result, the efficiency of anion–anion electrostatic repulsion was restricted, which in turn prevented the entry of water molecules.[4] Weak hydrogen bonds were generated between carboxyl groups at the same time, thus produced an additional physical crosslinking in the network, which inhibited the permeation of water molecules into the network.[29] Also, an enhancement of the water absorbency was

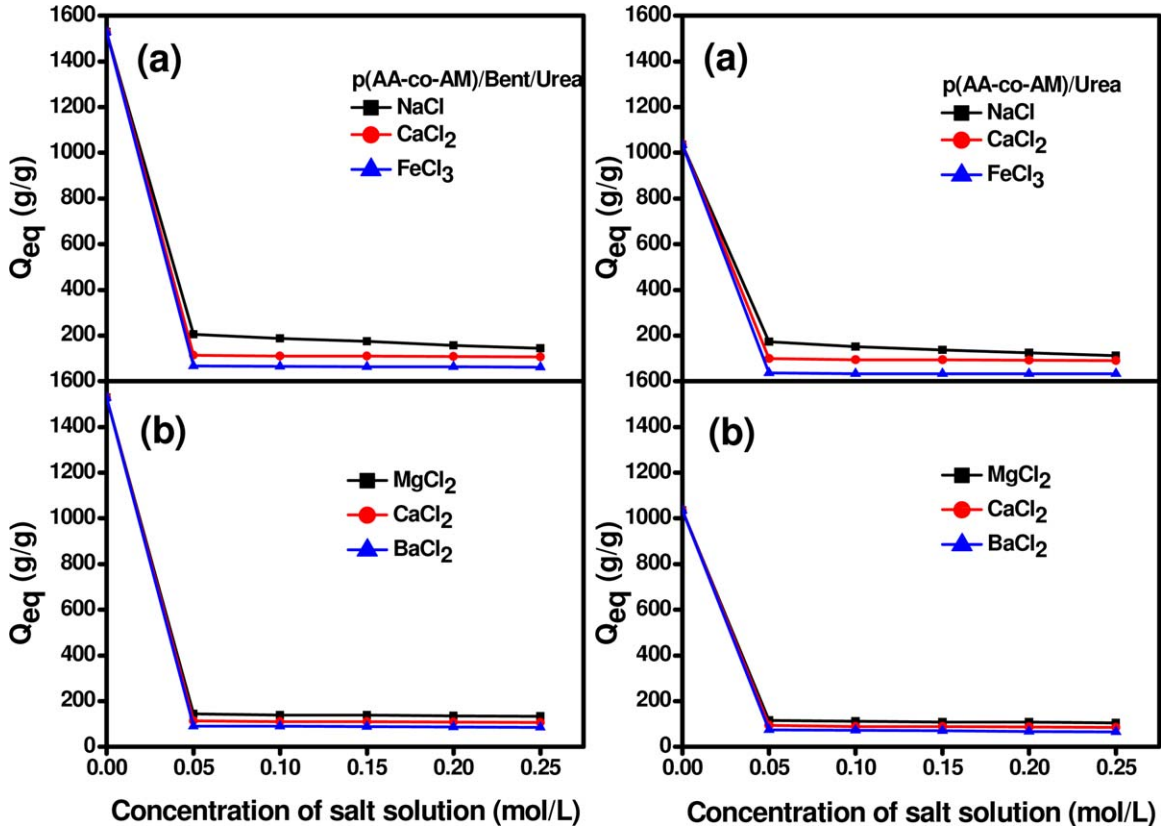

Figure 7. Effect of various ions and concentrations on the water absorbency of fertilizers. [Color figure can be viewed in the online issue, which is available at wileyonlinelibrary.com.]

noticed in the pH range of 4–8. This result may be explained by the fact that some carboxyl groups were ionized and converted into carboxylate anions that repelled one another and resulted in a rapid relaxation in the network chains, which eventually were conducive to the inclusion of water molecules into the network and increased swelling capacity.[4] However, a decrement was observed beyond pH 8, which may be related to the fact that the quantity of Na^+ cations from NaOH in the solution increased with an increase in the pH of swelling medium and then shielded the carboxylate anion groups. This occurrence prevented perfect anion–anion repulsion, which in turn shrunk the network and restricted the entry of water molecules.[4] Similar swelling-pH dependencies have been reported by others.[7,22]

Effect of Temperature on Water Absorbency. Temperature plays an extremely important part in water absorbency. Therefore, the swelling behaviors of p(AA-co-AM)/Urea and p(AA-co-AM)/Bent/Urea were investigated at various temperatures in distilled water and the results were shown in Figure 9, which implied that the water absorbency of p(AA-co-AM)/Bent/Urea was always higher than that of p(AA-co-AM)/Urea and with increasing temperature, all curves displayed the same tendency. Initially, water absorbency increased with an increase in temperature, and then decreased with a further increase in temperature. This result was attributed to the fact that higher temperature resulted in both greater diffusion of water molecules and larger relaxation of network chains.[8] In addition, the destruction of the hydrogen bonds between carboxyl groups facilitated network expansion,[30] which in turn improved the water absorbency of the samples. Hydrogen-bonding force, driving force for water entry, weakens when the temperature in the feed further increases, resulting in the bounded water in the composite network transforms into free water or nonbinding water and then moved rapidly out of the network.[31] Furthermore, the network structure shrinks with increasing temperature, which reduces the space into which water enters.[30] Both of

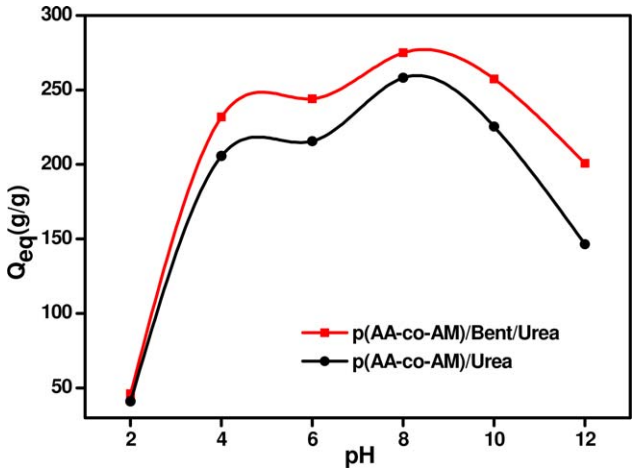

Figure 8. Effect of pH on the water absorbency of fertilizers. [Color figure can be viewed in the online issue, which is available at wileyonlinelibrary.com.]

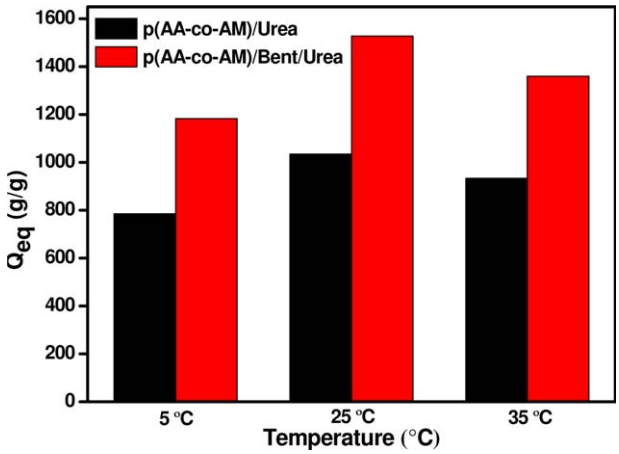

Figure 9. Effect of temperature on the water absorbency of fertilizers. [Color figure can be viewed in the online issue, which is available at wileyonlinelibrary.com.]

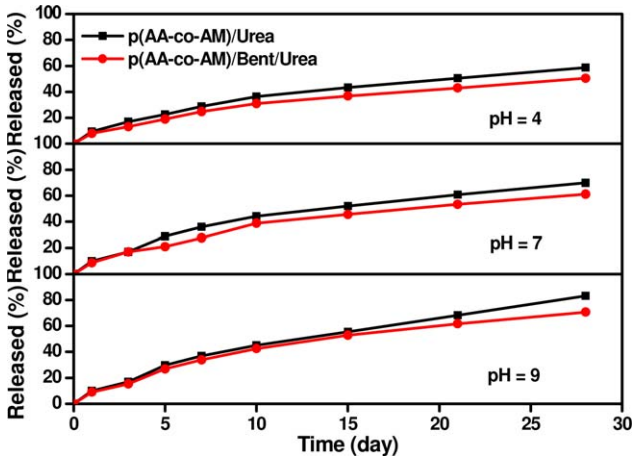

Figure 11. Release behavior of nutrients from fertilizers in solutions with different pH levels. [Color figure can be viewed in the online issue, which is available at wileyonlinelibrary.com.]

scenarios accounted for the decrease in water absorbency. A similar result was reported by Zhang *et al.*[30]

Influence of the Environmental Factors on the Release Behavior

Effect of Salt Solution on Release Behavior. The effect of salt solution type and concentration on release behavior was investigated and presented in Figure 10, which implies the salt solution types and concentrations prominently affect release behavior. It is noted that p(AA-co-AM)/Bent/Urea exhibited a slow release property that was superior to that of p(AA-co-AM)/Urea. This phenomenon was ascribed to the fact that the highly porous structure and the maze or tortuous path generated with the addition of Bent retarded the diffusion of fertilizer through the network to the medium.[4] As shown in Figure 10(a), the amounts of cumulative urea released from both two different samples in various salt solutions were appreciably

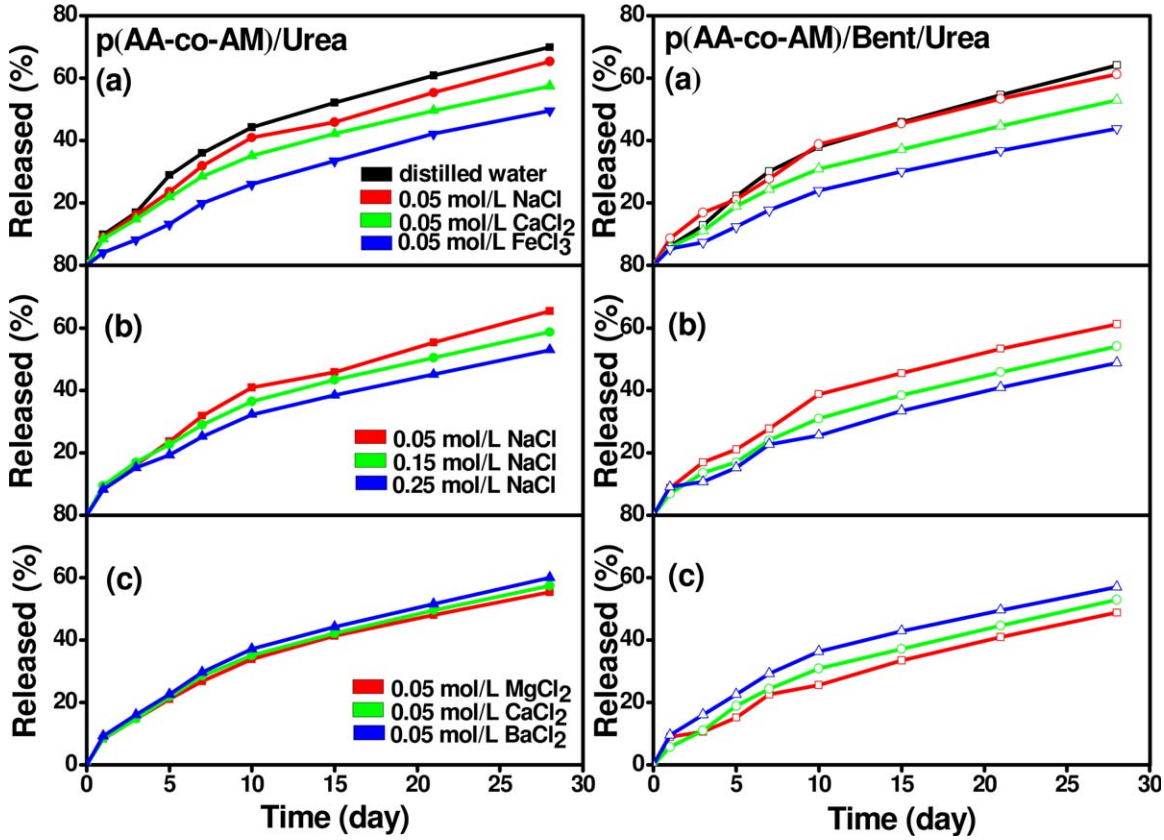

Figure 10. Effect of salt solution type and concentration on the release behavior of fertilizers. [Color figure can be viewed in the online issue, which is available at wileyonlinelibrary.com.]

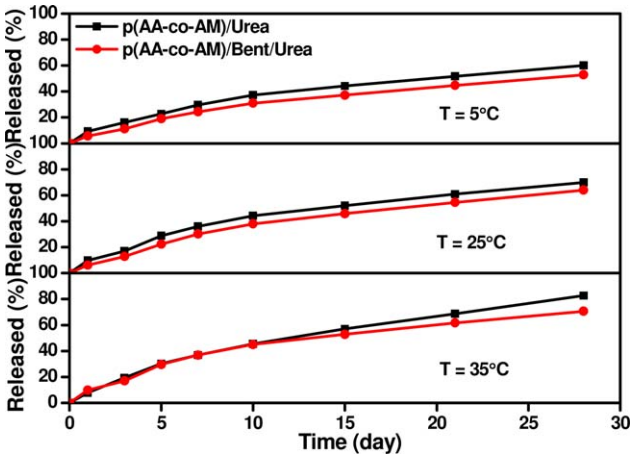

Figure 12. Release behavior of nutrients from fertilizers at different temperatures. [Color figure can be viewed in the online issue, which is available at wileyonlinelibrary.com.]

lower than that in distilled water, which is attributed to the charge screening effect of the additional cations and cause the perfect anion-anion electrostatic repulsion restricted in the process, subsequently the network shrunk and inhibited the release rate of nutrients.[27] The most remarkable is multivalent cations reduced release rate considerably more than monovalent cations did, which is related to the formation of intramolecular and intermolecular complexes due to the complexing ability between multivalent cations and the carboxylate groups, these complexes increased the cross-linking density of the network and caused the samples to become hard and rubbery, consequently, the amounts of nutrients released decreased as charge number increased.[27] As depicted in Figure 10(b), the release values decreased constantly with increasing concentration. These results can be explained by the fact that the charge screening effect and complexing ability were strengthened when concentration increased leading to a decrease in release amounts. As illustrated in Figure 10(c), the larger the radius of the cations, the higher the release amounts were. These results were related to the fact that the complexing ability between divalent cations and the carboxylate groups become weakened as the radius increased, consequently, crosslinking density decreased and the network relaxed, which led to an increase in the release amounts. On the basis of the discussion above, release behavior is strongly influenced by the type and concentration of salt solution added to the release medium.

Effect of pH on Release Behavior. Figure 11 shows the slow release behavior of nutrients from fertilizers in aqueous media at pH values of 4, 7, and 9 at room temperature. It is clearly seen that the release behaviors of the samples were sensitive to the environmental pH level. What should be noted is that the release rate of p(AA-co-AM)/Bent/Urea was slower than that of p(AA-co-AM)/Urea, indicating Bent can contribute to improving slow release behavior. The proposal was similar to the assertion mentioned above that the addition of Bent created a highly porous structure and a maze or tortuous path that restricted the release of urea into media. It is also found that the amount of nutrients released from the samples with widely varying rates and the release rate was increased with increasing pH level of the experiment conditions. The release rates for both samples were always higher in basic solution than in acidic or neutral solutions. These results were attributed to the deprotonation of the carboxylic groups in the basic solution, and the strong electrostatic repulsion between the carboxylic groups also make the network expand, which is convenient for the nutrients to pass through the network.[32] In contrast, the protonation of carboxylic groups at a low pH level prevented the efficient anion–anion electrostatic repulsion, and subsequently causes a shrinkage of the network, which is unfavorable for the transportation of nutrients.[33] Similar phenomena and results have been reported by Ma *et al.*[32]

Effect of Temperature on Release Behavior. The release behaviors of nutrients from the fertilizers in distilled water at temperatures of 5, 25, and 35°C were shown in Figure 12. It could be

Table I. The Release Kinetics Parameters *K*, *n*, and R^2 for p(AA-co-AM)/Urea and p(AA-co-AM)/Bent/Urea in Different Experimental Conditions

Experimental conditions	p(AA-co-AM)/urea			p(AA-co-AM)/bent/urea		
	R^2	*n*	*K*	R^2	*n*	*K*
0.05 mol L^{-1} NaCl	0.9902	1.6301	0.0283	0.9924	1.649	0.0289
0.05 mol L^{-1} $CaCl_2$	0.9935	1.6845	0.0279	0.9889	1.4538	0.0774
0.05 mol L^{-1} $FeCl_3$	0.992	1.2723	0.1769	0.9716	1.4206	0.1243
0.05 mol L^{-1} $MgCl_2$	0.9956	1.7158	0.0264	0.9515	1.7371	0.0342
0.05 mol L^{-1} $BaCl_2$	0.994	1.7329	0.0216	0.9931	1.8042	0.0174
0.15 mol L^{-1} NaCl	0.9969	1.791	0.0179	0.9946	1.5855	0.0478
0.25 mol L^{-1} NaCl	0.997	1.7652	0.0244	0.9515	1.7371	0.0342
pH = 4	0.9969	1.791	0.0179	0.9929	1.7405	0.0288
pH = 7	0.9832	1.6221	0.0246	0.9924	1.649	0.0289
pH = 9	0.9894	1.5175	0.0328	0.9847	1.5250	0.0367
T = 5°C	0.994	1.7329	0.0216	0.9889	1.4538	0.0774
T = 25°C	0.9832	1.6221	0.0246	0.9848	1.369	0.0797
T = 35°C	0.9891	1.4227	0.0464	0.9805	1.6066	0.0254

seen that temperature significantly influenced the release behaviors of nutrients and urea was released more slowly from p(AA-co-AM)/Bent/Urea than from p(AA-co-AM)/Urea at the same temperature in all tested temperature ranges. This result is reasonable on the basis of principle explained above, the introduction of Bent generated a highly porous structure and a maze or tortuous path, thus complicating the passage of urea through the network. Clearly, the higher the temperature, the faster the nutrient release rates were. The base fertilizer used in the experiment was urea, whose dissolution rate was increased with an increase in temperature. Moreover, diffusion rate increased as temperature increased because of a faster relaxation of network chains.[1,8,34] As per the discussion above, it is concluded that both of higher dissolution rate (due to the increased solubility of urea) and diffusion rate (originated from an accelerated relaxation of network chains) at high temperature enhanced nutrient release.[2] A similar result was presented by Tao *et al.*[2]

Slow Release Kinetics

For spherical matrices, when $n \leq 0.43$, the urea release mechanism approaches to a Fickian diffusion, whereas $n \geq 0.85$, Case II transport occurs, leading to a zero order (swelling or erosion controlled) release mechanism, and when $0.43 \leq n < 0.85$, anomalous transport is observed, involving both Fickian diffusion and polymer chain relaxation.[35] The values of K, n, and R^2 for nutrients released from p(AA-co-AM)/Urea and p(AA-co-AM)/Bent/Urea in different conditions were calculated and summarized in Table I. It was found that the release data had a good linear fit as shown by the values obtained for the correlation coefficients (R^2). It is also apparent that all diffusion exponent n were greater than 0.85 for both two fertilizers in all the cases, suggesting that release of urea was predominated by a Case II release mechanism with skeleton erosion.

CONCLUSIONS

A novel p(AA-co-AM)/Bent/Urea slow release fertilizer that contained 14.98% nitrogen was successfully prepared via free radical polymerization method. The results showed that the p(AA-co-AM)/Bent/Urea sample displayed exfoliated structures, good thermal stability and a micro-mesopores structure with more and consistent pore radius than p(AA-co-AM)/Urea sample did due to Bent reacting with AA and AM monomer by FTIR, XRD, TGA, SEM, and BET characterization. The swelling and release results in the different conditions revealed that swelling and release behavior was strongly dependent on the type and concentration of salt solution added to the media, as well as on solution pH levels and temperature. Therefore, the prepared samples exhibited excellent stimuli-responsive property to changes in external environment. The investigation into swelling and release behaviors indicated that the addition of Bent significantly increased water absorbency and water retention capacity and contributed considerably to improving the slow release behavior and endowed the product liberate the nutrient in a more controlled manner than that without Bent. The mechanism of urea release was based on a Case II release mechanism with skeleton erosion. Thus, the overall results would serve as a theoretical guide for the potential application of this fertilizer in agriculture and horticulture and contribute to the realization of sustainable development of agriculture.

ACKNOWLEDGMENTS

This study was financially supported by the National Natural Science Foundation of China (21466034). The author contributions are as follows: Conception and design: Peng Wen, Zhansheng Wu. Acquisition, analysis and interpretation of data: Peng Wen, Zhansheng Wu, Yanhui He. Manuscript writing and revision: Peng Wen, Zhansheng Wu, Yanhui He, Yajie Han, Yanbin Tong. Final approval of manuscript: Peng Wen, Zhansheng Wu, Yanhui He, Yajie Han, Yanbin Tong.

REFERENCES

1. Liang, R.; Liu, M.; Wu, L. *React. Funct. Polym.* **2007**, *6767*, 769.
2. Tao, S.; Liu, J.; Jin, K.; Qiu, X.; Zhang, Y.; Ren, X.; Hu, S. *J. Appl. Polym. Sci.* **2011**, *120*, 2103.
3. Wang, Y.; Liu, M.; Ni, B.; Xie, L.; Zhang, X. *J. Macromol. Sci. A* **2011**, *48*, 806.
4. Rashidzadeh, A.; Olad, A. *Carbohydr. Polym.* **2014**, *114*, 269.
5. Wu, L.; Liu, M.; Liang, R. *Bioresour. Technol.* **2008**, *99*, 547.
6. Qin, S.; Wu, Z.; Rasool, A.; Li, C. *J. Appl. Polym. Sci.* **2012**, *126*, 1687.
7. Rashidzadeh, A.; Olad, A.; Salari, D.; Reyhanitabar, A. *J. Polym. Res.* **2014**, *21*, 344.
8. Mishra, S.; Bajpai, J.; Bajpai, A. K. *J. Appl. Polym. Sci.* **2004**, *94*, 1815.
9. Al, E.; Güçlü, G.; İyim, T. B.; Emik, S.; Özgümüş, S. *J. Appl. Polym. Sci.* **2008**, *109*, 16.
10. Zheng, Y.; Cao, T.; Wang, A. *Ind. Eng. Chem. Res.* **2008**, *47*, 1766.
11. Bhattacharya, S. S.; Sen, K. K.; Sen, S. O.; Banerjee, S.; Kaity, S.; Ghosh, A. K.; Ghosh, A. *Int. J. Polym. Mater.* **2011**, *60*, 1015.
12. Sun, X.; Li, C.; Wu, Z.; Xu, X.; Ren, L.; Zhao, H. *Chin. J. Chem. Eng.* **2007**, *15*, 632.
13. With, T. K.; Petersen, T. D.; Petersen, B. *J. Clin. Pathol.* **1961**, *14*, 202.
14. Ritger, P. L.; Peppas, N. A. *J. Controlled Release* **1987**, *55*, 37.
15. He, Y.; Wu, Z.; Tu, L.; Han, Y.; Zhang, G.; Li, C. *Appl. Clay Sci.* **2015**, *109110*, 68.
16. Castro-Enríquez, D.; Rodríguez-Félix, F.; Ramírez-Wong, B.; Torres-Chávez, P.; Castillo-Ortega, M.; Rodríguez-Félix, D.; Armenta-Villegas, L.; Ledesma-Osuna, A. *Materials* **2012**, *5*, 2903.
17. He, X.; Liao, Z.; Huang, P.; Duan, J.; Ge, R.; Li, H.; Geng, Z. *Agric. Sci. China* **2007**, *6*, 338.
18. Li, J.; Hu, Y.; Pu, L.; Guo, G.; Niu, H. *Adv. Mater. Res.* **2014**, *1015*, 346.
19. Owens, D. E.; Jian, Y.; Fang, J. E.; Slaughter, B. V.; Chen, Y. H.; Peppas, N. A. *Macromolecules* **2007**, *40*, 7306.

20. Costa, M. M.; Cabral-Albuquerque, E. C.; Alves, T. L.; Pinto, J. C.; Fialho, R. L. *J. Agric. Food Chem.* **2013**, *61*, 9984.
21. Pereira, E. I.; Minussi, F. B.; da Cruz, C. C.; Bernardi, A. C.; Ribeiro, C. *J. Agric. Food Chem.* **2012**, *60*, 5267.
22. Pourjavadi, A.; Doulabi, M.; Soleyman, R.; Sharif, S.; Eghtesadi, S. A. *React. Funct. Polym.* **2012**, *72*, 667.
23. Zhang, M.; Cheng, Z.; Zhao, T.; Liu, M.; Hu, M.; Li, J. *J. Agric. Food Chem.* **2014**, *62*, 8867.
24. Kruk, M.; Jaroniec, M. *Chem. Mater.* **2001**, *13*, 3169.
25. Huang, L.; Sun, Y.; Yang, T.; Li, L. *Desalination* **2011**, *268*, 12.
26. Zhou, Y.; Fu, S.; Zhang, L.; Zhan, H. *Carbohydr. Polym.* **2013**, *97*, 429.
27. Sadeghi, M.; Hosseinzadeh, H. *Turk. J. Chem.* **2008**, *32*, 375.
28. Zhao, Y.; Su, H.; Fang, L.; Tan, T. *Polymer* **2005**, *46*, 5368.
29. Wang, W.; Wang, J.; Kang, Y.; Wang, A. *Compos. Part B-Eng.* **2011**, *42*, 809.
30. Zhang, X. Z.; Yang, Y. Y.; Wang, F. J.; Chung, T. S. *Langmuir* **2002**, *18*, 2013.
31. Lee, W. F.; Chen, C. F. *J. Appl. Polym. Sci.* **1998**, *69*, 2021.
32. Ma, Z.; Jia, X.; Zhang, G.; Hu, J.; Zhang, X.; Liu, Z.; Wang, H.; Zhou, F. *J. Agric. Food Chem.* **2013**, *61*, 5474.
33. Kenawy, E. R.; Sakran, M. A. *Ind. Eng. Chem. Res.* **1996**, *35*, 3726.
34. Tomaszewska, M.; Jarosiewicz, A. *J. Agric. Food. Chem.* **2002**, *50*, 4634.
35. Kaygusuz, H.; Erim, F. B. *React. Funct. Polym.* **2013**, *73*, 1420.